Porous metal-organic frameworks with 5-aminoisophthalic acid as platforms for functional applications about high photodegradation efficiency of phenol

Ying Wang[a], Li-Jing Zhang[a], Rui Zhang[c], Yu Jin[a], Yang Wang[a], Yong-Heng Xing[a,*], Feng-Ying Bai[a,*], Li-Xian Sun[b]

[a] College of Chemistry and Chemical Engineering, Liaoning Normal University, Huanghe Road 850#, Dalian 116029, P. R. China.

[b] Guangxi Key Laboratory of Information Materials, Guilin University of Electronic Technology, Guilin 541004, P. R. China.

[c] Dandong Second Middle School, Rejuvenation Area Yingcai Street 2#, Dandong 118000, P. R. China.

E-mail: xingyongheng2000@163.com (Yong-Heng Xing);

E-mail: baifengying2003@163.com (Feng-Ying Bai);

Supplementary Index

Materials and methods

Ligand L and all others chemicals purchased commercially were of reagent grade or better and used without further purification. All IR measurements were obtained using a Bruker AXS TENSOR-27 FT-IR spectrometer with pressed KBr pellets in the range of 400-4000 cm^{-1} at room temperature. UV-Vis-NIR spectra for complexes **1-4** and the L ligand were recorded on a JASCO V-570 UV/Vis/NIR microspectrophotometer (200-2500 nm). Elemental analyses of C, H and N were conducted on a PerkinElmer 240C automatic analyzer. Thermogravimetric analysis (TG) was performed on a PerkinElmer Diamond TG/DTA under atmosphere from room temperature to 1000 °C with a heating rate of 10 °C/min. Powder X-ray diffraction pattern was obtained on a Advance-D8 equipped with Cu Ka radiation in the range $5° < 2\theta < 55°$, with a step size of 0.02° (2θ) and a count time of 2 s/step.

X-ray crystallographic determination

Suitable single crystals of the four complexes were mounted on glass fibers for X-ray measurement, respectively. Reflection data were collected at room temperature on a Bruker AXS SMART APEX II CCD diffractometer with graphite monochromatized Mo-Kα radiation (λ = 0.71073 Å). All the measured independent reflections ($I > 2\sigma(I)$) were used in the structural analyses, and semi-empirical absorption corrections were applied using the SADABS program. The structure was solved by direct methods using the SHELX-97 program. All non-hydrogen atoms were refined anisotropically. The hydrogen atoms of the organic frameworks were geometrically fixed at calculated positions and refined using a riding model. The crystallographic data for complexes **1-4** are given in **Table S1**. The selected bond distances (Å) of complexes **1-4** are given in **Table S2**.

The research methods and experimental data on photocatalytic degradation

In the experiment of photocatalytic degradation of phenol, at 25 °C, using mercury lamp as the ultraviolet light source (λ = 254 nm, 220 V, 18 W). First, prepare 250 mL of the phenol solution and add 0.05 g of the complex to the phenol solution while adding 0.5 ml of a buffer solution of pH = 10, 1.0 ml of potassium ferricyanide at a mass fraction of 8%, and 1.0 ml of a 4-aminoantipyrine solution with a mass fraction of 2%. Mixed evenly, placed in the reactor for

UV degradation reaction. After 20 min, remove about 4 mL of the suspension, centrifuged at 2500 r/min for 3 min to take the supernatant. The absorbance curve (scanning range 400~700 nm) was scanned with a UV-1000 single-beam UV/Vis spectrophotometer and the absorbance at the maximum absorption wavelength (λ_{max} = 505 nm) was recorded. And then repeat the operation every 20 min. The absorption wavelength (λ) and the absorbance (A) curve can be obtained.

The detailed experimental conditions for using an HPLC instrument

The degradation intermediates from phenol were monitored using an HPLC instrument of the LC-6A series (Shimadzu Company, Japan) equipped with an YMC-C18 column (250 mm × 46 mm, 5 μm). During sample analysis, the column was maintained at 25 °C. The intermediates were detected using an isocratic elution program. Acetonitrile and water with a volume ratio of 50: 50 were used as the mobile phase at a flow-rate of 0.8 $mL \cdot min^{-1}$ and the injection volume was 20 μL.

Table S1. The crystallographic data for complexes **1-4**

Complexes	**1**	**2**	**3**	**4**
Formula	$C_8H_8NO_5Co$	$C_8H_8NO_5Zn$	$C_{16}H_{20}N_2O_{12}Ni$	$C_8H_9NO_6Cd$
M ($g \cdot mol^{-1}$)	257.08	263.52	491.05	327.56
Crystal system	*Monoclinic*	*Monoclinic*	*Monoclinic*	*Monoclinic*
Space group	$P2_1/c$	$P2_1/n$	$C2/c$	$P2_1/n$
a (Å)	8.8157(7)	9.0381(11)	14.2285(16)	10.2605(8)
b (Å)	12.5671(10)	8.2616(10)	11.1581(12)	7.2802(6)
c (Å)	7.9788(6)	11.6301(14)	12.6109(14)	12.8133(10)
α (°)	90	90	90	90
β (°)	97.4870(10)	100.868(2)	113.559(2)	90.7570(10)
γ (°)	90	90	90	90
V ($Å^3$)	876.42(12)	852.83(18)	1835.3(4)	957.05(13)
Z	4	4	4	4
D_c ($g \cdot cm^{-3}$)	1.948	2.052	1.777	2.273
F(000)	520	532	1016	640
M(Mo Kα) (mm^{-1})	1.958	2.879	1.132	2.295
θ (°)	2.33-28.29	2.63-26.00	2.40-25.98	2.53-25.00
Reflections collected	6401	4560	4974	4700

Independent reflections($I>2\sigma(I)$)	2178(1834)	1679(1566)	1799(1537)	1682(1438)
Parameters	136	136	143	145
$\Delta(\rho)$(e Å^{-3})	0.352 and -0.402	0.381 and -0.398	0.498 and -0.390	0.491 and -0.553
Goodness of fit on F^2	1.051	1.054	1.091	0.646
R^a	0.0287(0.0371)[b]	0.0203(0.0221)[b]	0.0304(0.0366)[b]	0.0237(0.0318)[b]
wR_2[a]	0.0657(0.0699)[b]	0.0592(0.0600)[b]	0.0893(0.0922)[b]	0.0530(0.0551)[b]

*[a]$R=\sum \left| F_O-F_C \right| / \sum \left| F_O \right|$, $wR_2=\{\sum[w(F_O^2-F_C^2)^2]/\sum[w(F_O^2)^2]\}^{1/2}$; [$F_O>4\sigma(F_O)$]. [b]Based on all data.

Table S2. The selected bond distances (Å) of complexes **1-4**

Complex **1**			
Co(1)-O(1)	2.0180(15)	Co(1)-O(4)$^{\#2}$	2.1198(14)
Co(1)-O(2)$^{\#1}$	1.9892(15)	Co(1)-O(6)	2.1073(16)
Co(1)-O(3)$^{\#2}$	2.2619(15)	Co(1)-N(1)$^{\#3}$	2.2233(18)
Complex **2**			
Zn(1)-O(2)	1.9587(14)	Zn(1)-O(5)	1.9653(15)
Zn(1)-O(4)$^{\#1}$	1.9779(13)	Zn(1)-N(1)$^{\#2}$	2.0364(16)
Complex **3**			
Ni(1)-O(3)$^{\#2}$	2.0776(15)	Ni(1)-O(5)$^{\#1}$	2.0618(17)
Ni(1)-O(3)$^{\#3}$	2.0776(15)	Ni(1)-N(1)	2.1506(18)
Ni(1)-O(5)	2.0618(17)	Ni(1)-N(1)$^{\#1}$	2.1506(18)
Complex **4**			
Cd(1)-O(2)	2.230(2)	Cd(1)-O(4)$^{\#2}$	2.479(2)
Cd(1)-O(3)$^{\#2}$	2.333(2)	Cd(1)-O(5)	2.362(3)
Cd(1)-O(3)$^{\#3}$	2.589(3)	Cd(1)-N(1)$^{\#1}$	2.254(3)

*Symmetry codes: complex **1**: #1 -x,-y+1,-z+2; #2 -x+1,y-1/2,-z+5/2; #3 x,-y+3/2,z+1/2; complex **2**: #1 x+1/2,-y+3/2,z-1/2; #2 x+1/2,-y+1/2,z-1/2; complex **3**: #1 -x+1/2,-y+1/2,-z; #2 -x+1/2,y-1/2,-z+1/2; #3 x,-y+1,z-1/2; complex **4**: #1 x+1/2,-y+1/2,z+1/2; #2 x+1,y,z; #3 -x,-y,-z+1.

Table S3. The absorbance values of different concentrations of phenol solution

C(mg/L)	0	0.2	0.6	1	1.4	1.8	2.2	2.6
Abs	0	0.007	0.0173	0.0311	0.0404	0.0517	0.0613	0.0739

PXRD spectra:

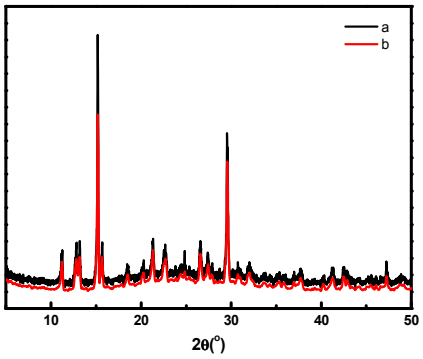

(a)

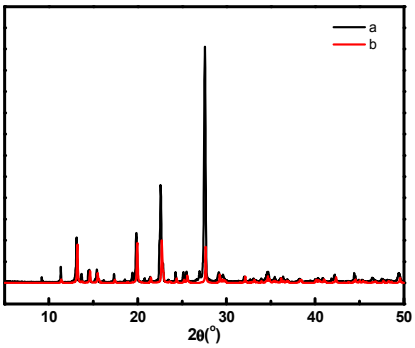

(b)

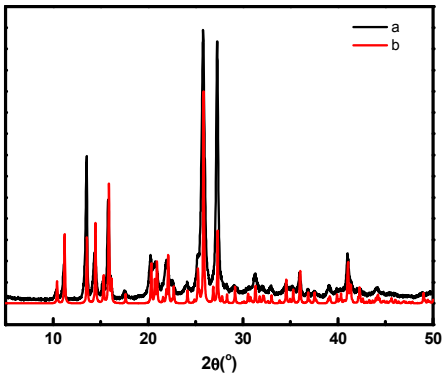

(c)

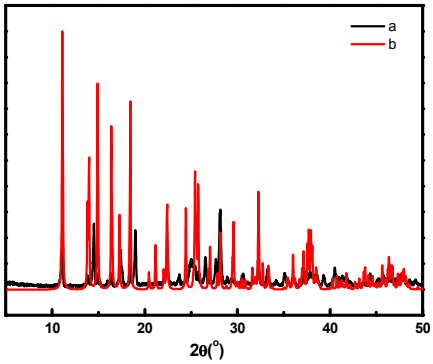

(d)

Figure S1. The PXRD spectra: (a) complex **1**; (b) complex **2**; (c) complex **3**; (d) complex **4**

IR spectra:

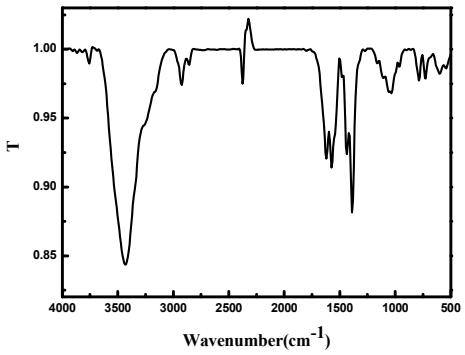

(a)

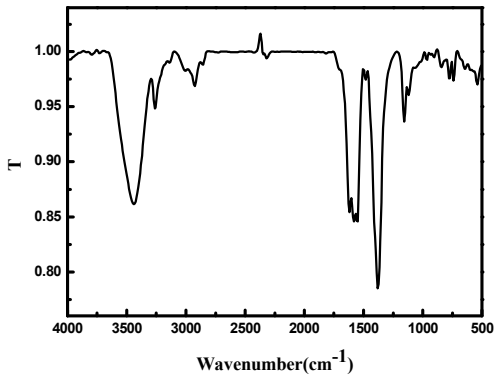

(b)

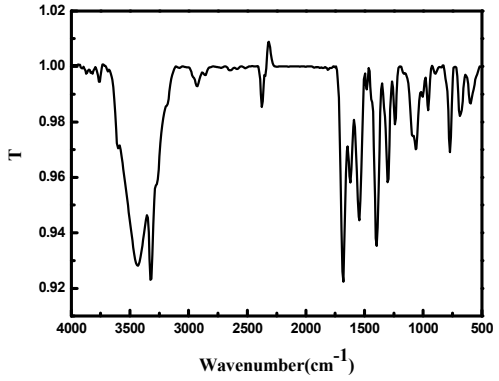

(c)

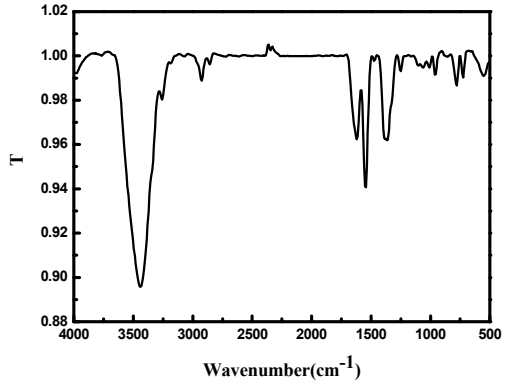

(d)

Figure S2. The IR spectra: (a) complex **1**; (b) complex **2**; (c) complex **3**; (d) complex **4**

UV-Vis spectra:

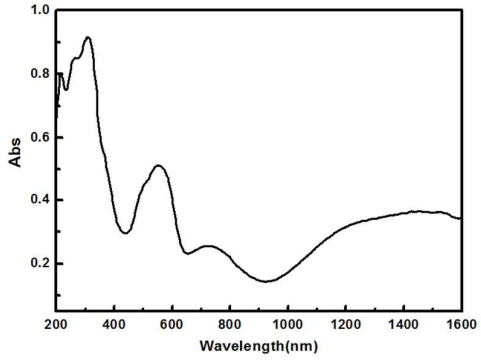

(a)

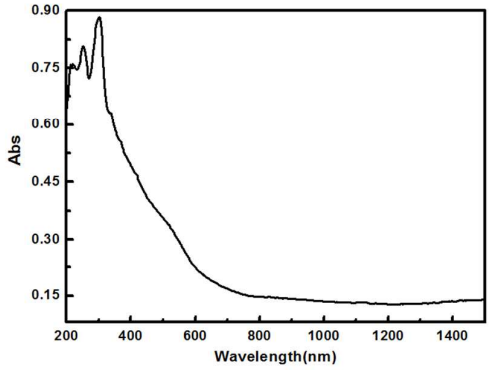

(b)

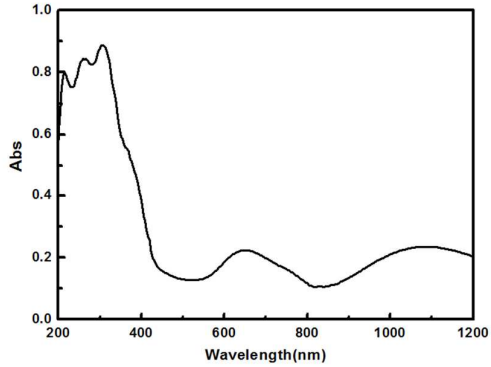

(c)

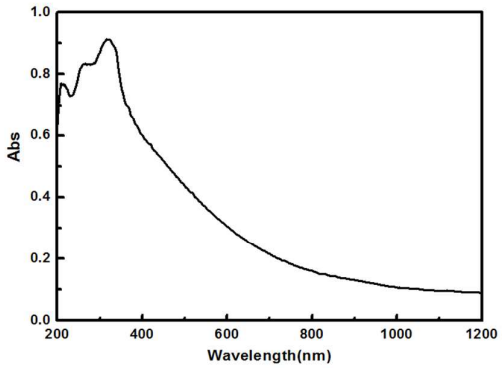

(d)

Figure S3. The UV-Vis spectra: (a) complex **1**; (b) complex **2**; (c) complex **3**; (d) complex **4**

TG spectra:

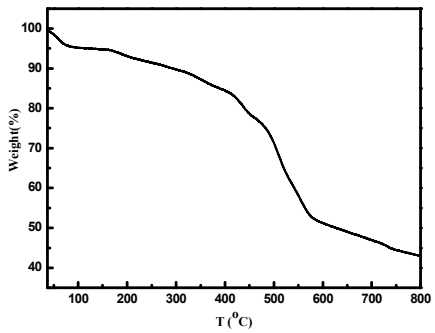

(a)

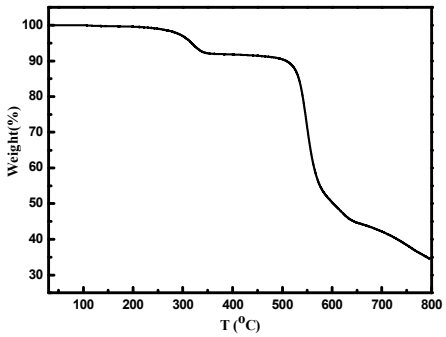

(b)

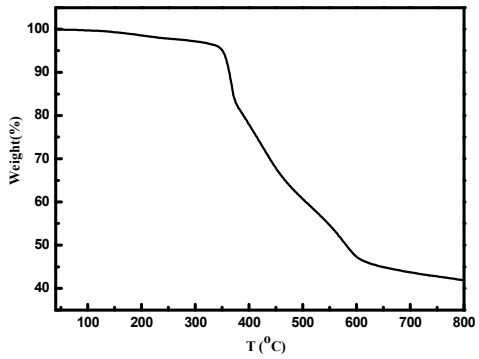

(c)

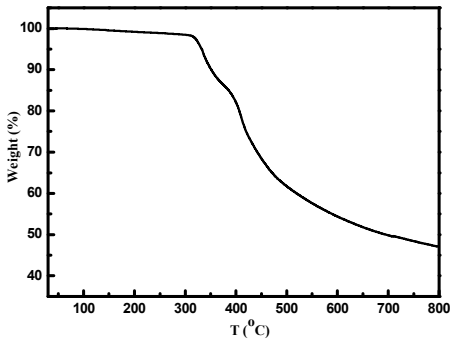

(d)

Figure S4. The TG spectra: (a) complex **1**; (b) complex **2**; (c) complex **3**; (d) complex **4**

Standard curve of phenol:

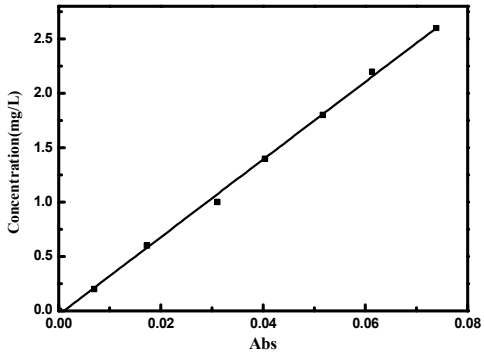

Figure S5. Standard curve of phenol

Dynamics model:

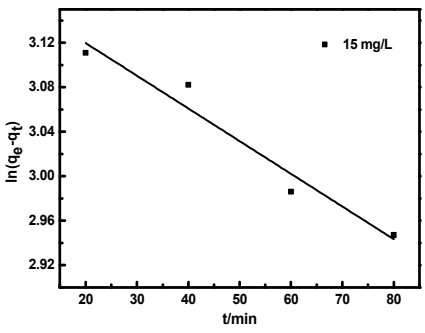

(a)

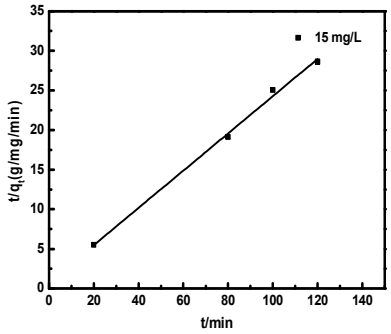

(d)

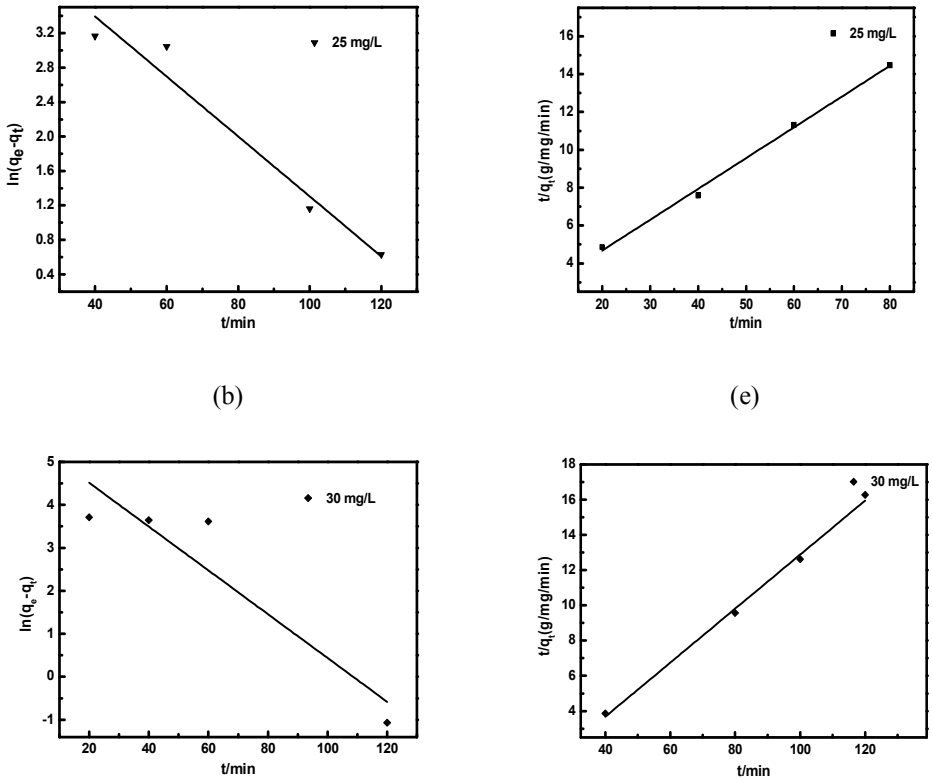

Figure S6. Pseudo-first-order dynamics model: (a) 15 mg/L; (b) 25 mg/L; (c) 30 mg/L; Pseudo-second-order dynamics model: (d) 15 mg/L; (e) 25 mg/L; (f) 30 mg/L

Phenol, phenol and diphenols mixtures of HPLC:

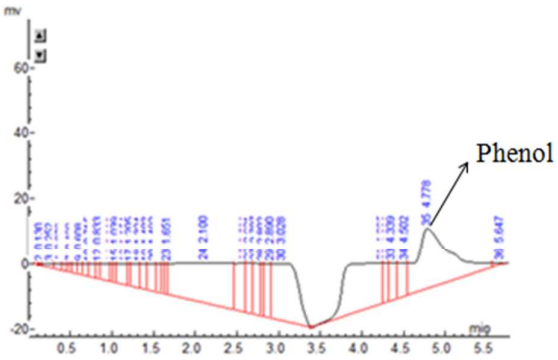

(a)

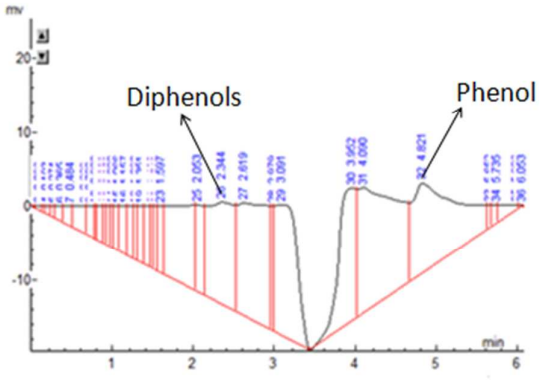

(b)

Figure S7. HPLC: (a) Phenol; (b) Phenol and diphenols mixtures

HPLC in the course of experiment:

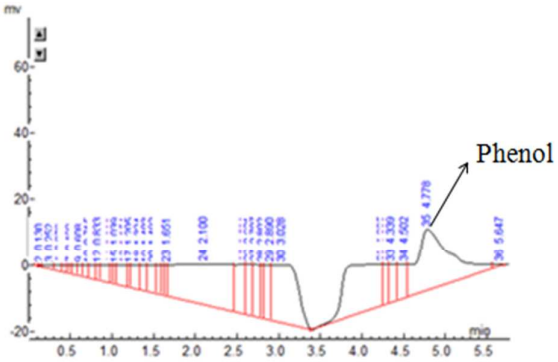

(a)

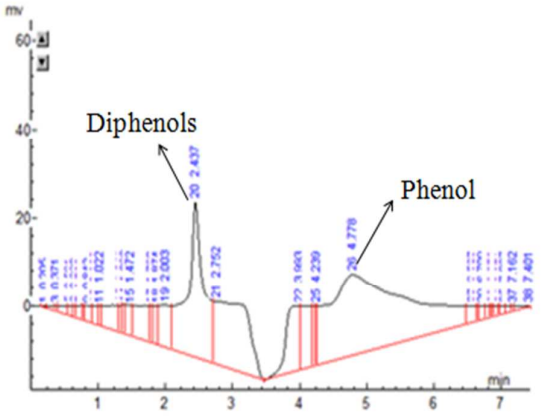

(b)

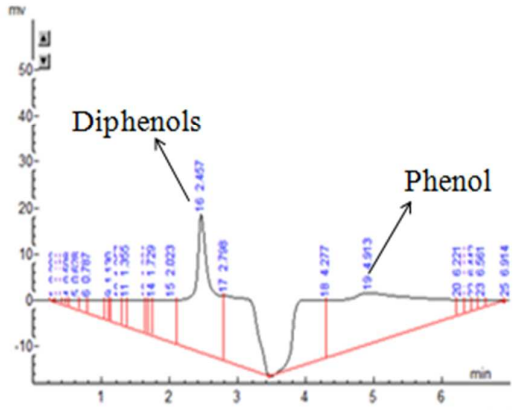

(c)

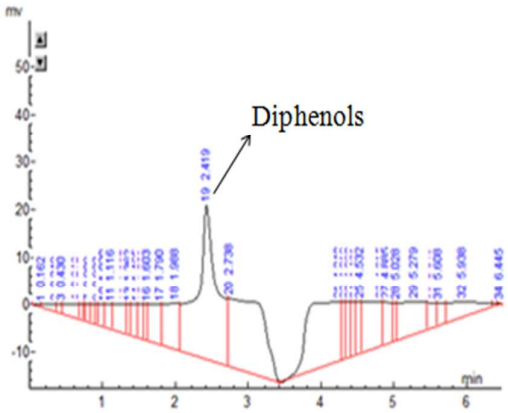

(d)

Figure S8. HPLC in the course of experiment: (a) 0 min; (b) 40 min; (c) 80 min; (d) 120 min

Comparison of PXRD before and after adsorption:

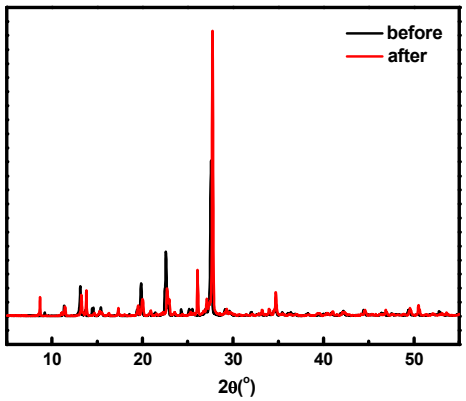

Figure S9. The PXRD spectra before and after phenol adsorption

The degradation efficiency of the regeneration cycle (three times):

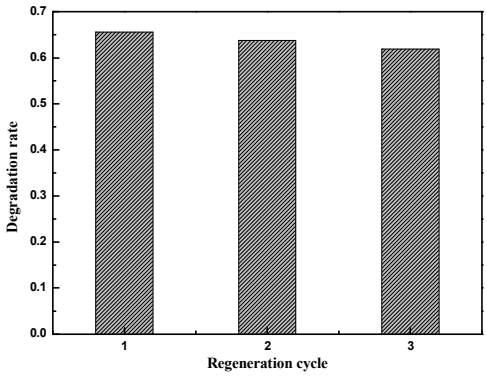

Figure S10. The degradation efficiency of the regeneration cycle